Electronic Supplementary Material (ESI) for Dalton Transactions.

Structures and Magnetic Properties of Dysprosium Complexes: the Effect of Crystallization Temperature

Mei Guo,[a,b] Yue Wang,[a] Jianfeng Wu,[a,b] Lang Zhao,[a] and Jinkui Tang*[a]

[a]State Key Laboratory of Rare Earth Resource Utilization, Changchun Institute of Applied Chemistry, Chinese Academy of Sciences, Changchun 130022, P. R. China. E-mail: tang@ciac.ac.cn

[b]University of Chinese Academy of Science, Beijing 100049, P. R. China

Table S1 Selected bond lengths (Å) and bond angles (°) of **1**.

Dy(1)-O(2)	2.353(7)	O(8)-Dy(1)-O(10)	99.2(3)
Dy(1)-O(3)	2.231(7)	O(3)-Dy(1)-N(2)	71.2(3)
Dy(1)-O(14)	2.360(10)	O(2)-Dy(1)-N(2)	64.3(3)
Dy(1)-O(13)	2.369(10)	O(14)-Dy(1)-N(2)	72.6(3)
Dy(1)-O(8)	2.481(8)	O(13)-Dy(1)-N(2)	80.7(3)
Dy(1)-O(10)	2.497(8)	O(8)-Dy(1)-N(2)	132.4(3)
Dy(1)-N(2)	2.499(9)	O(10)-Dy(1)-N(2)	127.1(3)
Dy(1)-O(11)	2.513(8)	O(3)-Dy(1)-O(11)	155.5(2)
Dy(1)-O(7)	2.527(9)	O(2)-Dy(1)-O(11)	69.8(3)
O(3)-Dy(1)-O(2)	133.6(3)	O(14)-Dy(1)-O(11)	77.5(3)
O(3)-Dy(1)-O(14)	95.9(3)	O(13)-Dy(1)-O(11)	120.7(3)
O(2)-Dy(1)-O(14)	83.5(3)	O(8)-Dy(1)-O(11)	71.8(3)
O(3)-Dy(1)-O(13)	74.9(3)	O(10)-Dy(1)-O(11)	50.7(3)
O(2)-Dy(1)-O(13)	85.2(3)	N(2)-Dy(1)-O(11)	127.0(3)
O(14)-Dy(1)-O(13)	153.2(3)	O(3)-Dy(1)-O(7)	77.4(3)
O(3)-Dy(1)-O(8)	83.8(3)	O(2)-Dy(1)-O(7)	141.0(3)
O(2)-Dy(1)-O(8)	137.2(3)	O(14)-Dy(1)-O(7)	121.4(3)
O(14)-Dy(1)-O(8)	70.4(3)	O(13)-Dy(1)-O(7)	81.7(3)
O(13)-Dy(1)-O(8)	131.5(3)	O(8)-Dy(1)-O(7)	51.0(3)
O(3)-Dy(1)-O(10)	135.8(3)	O(10)-Dy(1)-O(7)	71.2(3)
O(2)-Dy(1)-O(10)	69.8(3)	N(2)-Dy(1)-O(7)	147.1(3)
O(14)-Dy(1)-O(10)	126.9(3)	O(11)-Dy(1)-O(7)	85.9(3)
O(13)-Dy(1)-O(10)	70.5(3)		

Table S2 Selected bond lengths (Å) and bond angles (°) of **2**.

Dy(1)-O(4)#1	2.253(6)	O(10)-Dy(1)-O(7)	76.8(2)
Dy(1)-O(13)	2.324(7)	O(4)#1-Dy(1)-O(8)	147.6(2)
Dy(1)-O(2)	2.354(6)	O(13)-Dy(1)-O(8)	76.5(2)
Dy(1)-O(5)#1	2.374(7)	O(2)-Dy(1)-O(8)	72.6(2)
Dy(1)-O(10)	2.447(7)	O(5)#1-Dy(1)-O(8)	71.1(2)
Dy(1)-O(7)	2.471(6)	O(10)-Dy(1)-O(8)	123.7(2)

Dy(1)-O(8)	2.502(7)	O(7)-Dy(1)-O(8)	51.7(2)
Dy(1)-N(1)#1	2.509(9)	O(4)#1-Dy(1)-N(1)#1	70.1(2)
Dy(1)-O(11)	2.533(7)	O(13)-Dy(1)-N(1)#1	140.6(2)
O(4)#1-Dy(1)-O(13)	79.3(2)	O(2)-Dy(1)-N(1)#1	74.4(2)
O(4)#1-Dy(1)-O(2)	81.3(2)	O(5)#1-Dy(1)-N(1)#1	64.6(2)
O(13)-Dy(1)-O(2)	77.1(2)	O(10)-Dy(1)-N(1)#1	80.2(2)
O(4)#1-Dy(1)-O(5)#1	132.8(2)	O(7)-Dy(1)-N(1)#1	135.1(2)
O(13)-Dy(1)-O(5)#1	147.1(2)	O(8)-Dy(1)-N(1)#1	118.9(3)
O(2)-Dy(1)-O(5)#1	98.3(2)	O(4)#1-Dy(1)-O(11)	74.6(2)
O(4)#1-Dy(1)-O(10)	87.7(2)	O(13)-Dy(1)-O(11)	72.2(2)
O(13)-Dy(1)-O(10)	123.4(3)	O(2)-Dy(1)-O(11)	143.8(2)
O(2)-Dy(1)-O(10)	154.5(2)	O(5)#1-Dy(1)-O(11)	118.0(2)
O(5)#1-Dy(1)-O(10)	72.7(2)	O(10)-Dy(1)-O(11)	51.3(3)
O(4)#1-Dy(1)-O(7)	145.3(2)	O(7)-Dy(1)-O(11)	71.4(2)
O(13)-Dy(1)-O(7)	83.7(2)	O(8)-Dy(1)-O(11)	116.9(2)
O(2)-Dy(1)-O(7)	123.9(2)	N(1)#1-Dy(1)-O(11)	120.1(2)
O(5)#1-Dy(1)-O(7)	71.9(2)		

Symmetry transformations used to generate equivalent atoms: #1 -x+2, -y+1, -z+1

Table S3 Lanthanide geometry analysis by SHAPE software for **1** and **2**.

Geometry	Capped square antiprism (C_{4v})	Spherical square capped antiprism (C_{4v})	Tricapped trigonal prism (D_{3h})	Spherical tricapped trigonal prism (D_{3h})
1	2.874	2.033	3.276	2.262
2	1.868	2.705	1.755	9.952

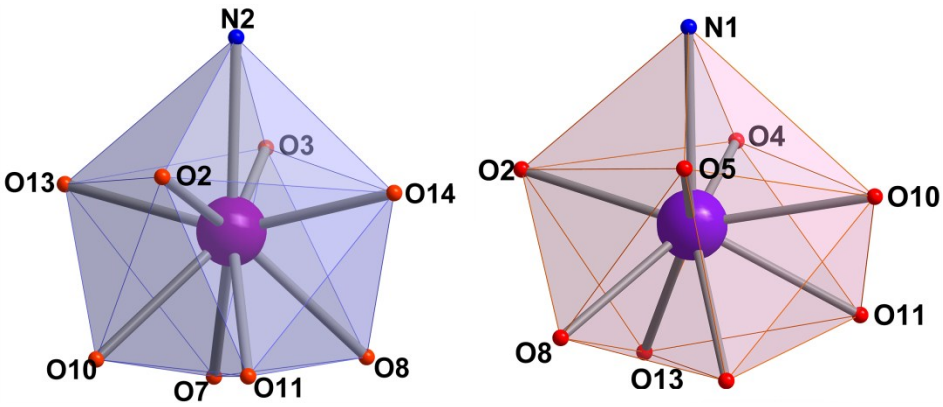

Fig. S1 The coordination sphere of Dy^{III} centers in **1** (left) and **2** (right), respectively.

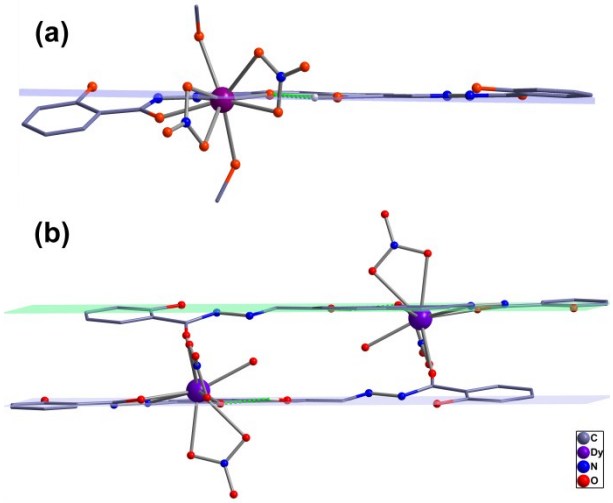

Fig. S2 (a) The plane of ligand in compound **1**; (b) Two planes of ligands in complex **2**.

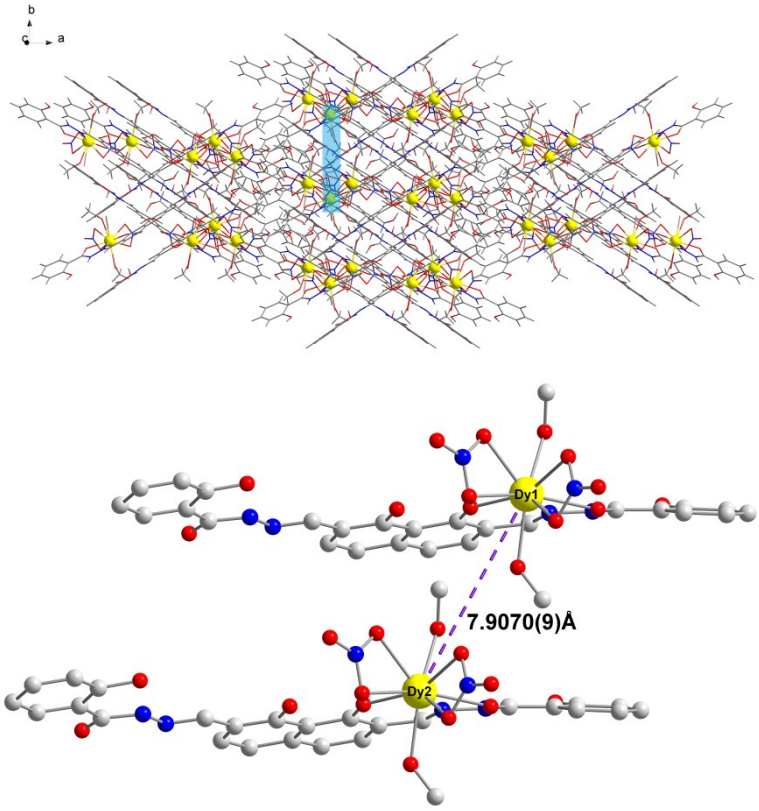

Fig. S3 Packing diagram of **1** viewed along the *c*-axis (top) and the diagram showing the shortest intermolecular Dy···Dy distance for **1** (bottom). Color code: yellow, Dy; red, O; blue, N; gray, C.

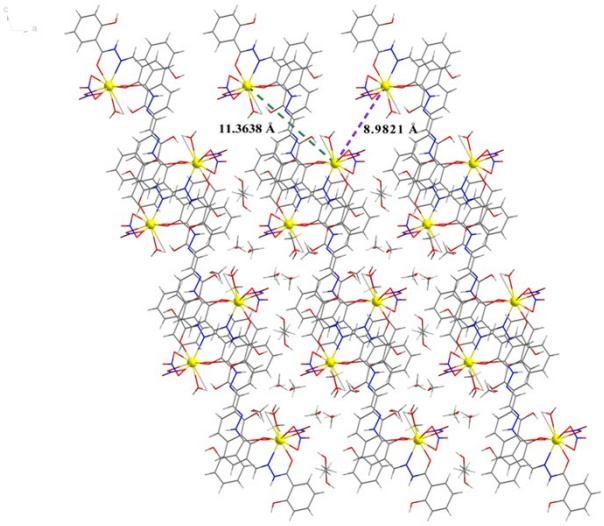

Fig. S4 Packing diagram of **2** viewed along the *c*-axis for **2**. Color code: yellow, Dy; red, O; blue, N; gray, C.

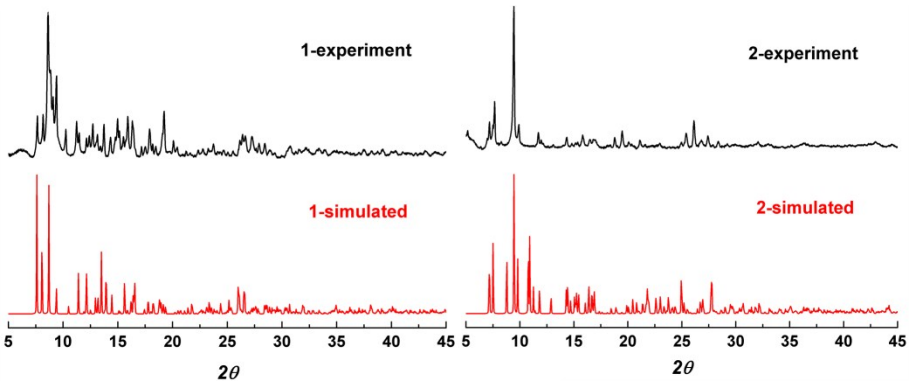

Fig. S5 Powder XRD analyses of complexes **1** (left) and **2** (right). The red line is simulated data from single crystal data.

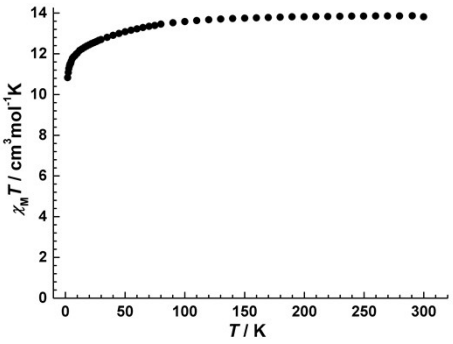

Fig. S6 Temperature dependence of the $\chi_M T$ product at 1000 Oe for **1.**

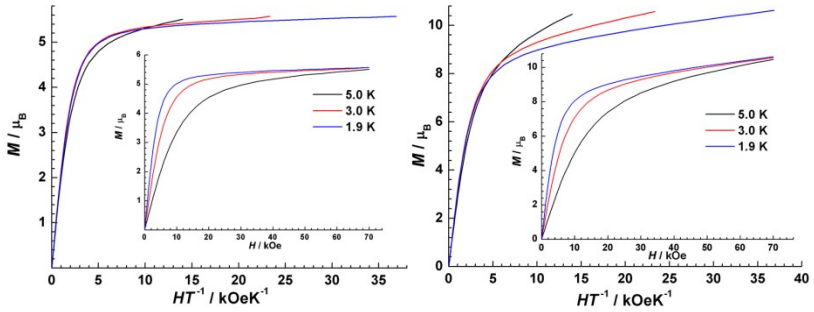

Fig. S7 *M* versus *H/T* plots at 1.9, 3.0, and 5 K for **1**(left) and **2**(right). Inset: Field dependence of the magnetization between 1.9 and 5 K for **1** and **2**.

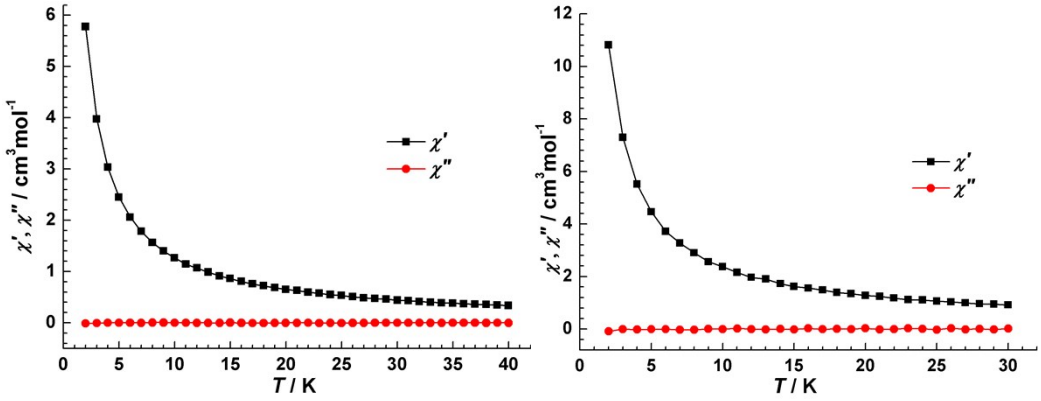

Fig. S8 Temperature dependence of the in-phase and out-of-phase ac susceptibility under 0 Oe dc field for **1** (left) and **2** (right).

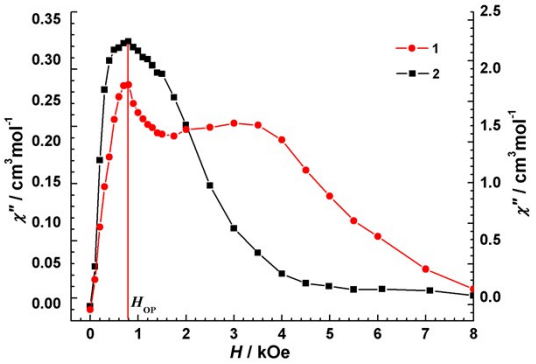

Fig. S9 Dependence of the out-of-phase signals of **1** and **2** on applied dc field strength at 1.9 K, 997 Hz.

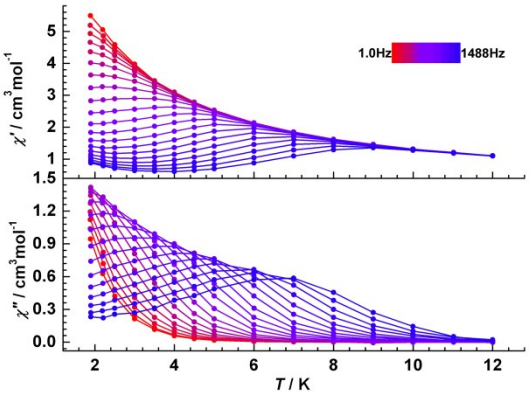

Fig. S10 Temperature dependence of the in-phase (top) and out-of-phase (bottom) ac susceptibility under 800 Oe dc field for **1**.

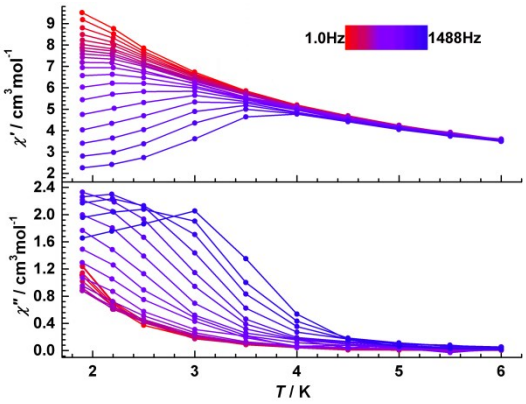

Figure S11. Temperature dependence of the in-phase (top) and out-of-phase (bottom) ac susceptibility under 1000 Oe dc field for **2**.